Novel force-based finite element formulation to predict axial force-bending moment interaction of RC frames and walls

Sameera S. Hippola[1a], Chathura M. Rakapakse[1b], Kushan K. Wijesundara[*1] and Ranjith Dissanayake[1c]

[1]Department of Civil Engineering, University of Peradeniya, Peradeniya, Sri Lanka

(Received , Revised , Accepted)

Abstract. The most popular method to perform nonlinear analysis of RC frames is force based fiber beam column element which has two nested iterative procedures at structure and element levels. In the element level iterative procedure, section residual deformations are integrated to find element residual deformations. Then a suitable element corrective force is calculated which is later distributed at section level using force interpolation functions. Subsequently, section residual deformations are computed again and integrated to find element residual deformations. This iterative procedure is continued until the element residual deformation comes inside a prescribed tolerance and yields corresponding element resisting forces for a given element nodal deformations. However, it should be noted that the existing force-based fiber beam column element formulation does not include an explicit method to consider section equilibrium. Therefore, this paper proposes a novel force based finite element formulation with an iterative procedure at section level to correct section residual deformations at section level itself, rather than transferring errors of section level to element level and deciding a correction globally. The proposed formulation was experimentally validated and was proved to be accurate and stable. The potential advantages of considering section level equilibrium were discussed towards the end.

Keywords: RC frames; nonlinear static analysis; force based fiber beam column element; axial force – bending moment interaction; section level equilibrium.

1. Introduction

Reinforced concrete structures should be designed to avoid the brittle failure mode, which tends to happen without prior warning leading to catastrophic consequences. Therefore, it is vital to predict the behavior of reinforced concrete structures and their elements quite accurately through nonlinear analysis, accounting for the geometric and material nonlinearities under extreme loading conditions. In general, there are three methods of modelling the nonlinear behavior of reinforced concrete structures namely, lumped plasticity method, distributed plasticity method with line elements and modelling with three dimensional solid elements. In lumped plasticity method, the analysis is performed by lumping the plastic behavior at predetermined locations of the structure. Rajasankar *et al.* (2009) have proposed a formulation to model plastic hinges of RC frames using continuum damage mechanics while Iu (2016) has utilized higher order elements with refined plastic hinges to model RC structures. More recently, Colangelo (2018) has tuned a lumped plasticity frame model with axial force-bending moment interaction and Tidemann and Krenk (2018) have in cooperated cyclic loads and local joint effects. Although the lumped plasticity method comparatively requires

∗Corresponding author, Ph.D., E-mail: kushanw@pdn.ac.lk
[a] MPhil Student, E-mail: samhipo@gmail.com
[b] Ph.D. Student, E-mail: chaturarajapakse@gmail.com
[c] Professor, E-mail: ranjith@fulbrightmail.org

the least computational effort, it is beset by practical problems such as predetermining the possible plastic hinge locations as well as the reduced accuracy of the solutions. On the other hand modelling a whole reinforced concrete structure using three dimensional solid elements can produce more accurate predictions. However, this requires a giant computational effort, which could be impractical for practicing engineer with the existing computer facilities. Distributed plasticity method with line elements provide a good compromise between the accuracy of results and the computational effort required. In this method, plasticity is monitored along the element with the aid of control stations or integration points. Therefore, recent studies have been inclined towards line element with distributed plasticity. First line elements with distributed plasticity were based on stiffness. Taucer *et al.* (1991) provides an extensive review on the models based on discrete finite elements.

In distributed plasticity method with line elements, the relationship between element nodal deformation and nodal force increments can be derived using displacement based, force based or mixed finite element formulation approaches. In displacement - based formulation, equilibrium is satisfied in weak form while compatibility and constitutive relationship are satisfied in strong form. It should be noted that the displacement based finite element approach assumes the variation of displacement along an element, in addition to the equilibrium, constitutive relationship and compatibility. However, in the force based finite element method, the internal forces along the element are known exactly through equilibrium equations. Therefore force based finite element method does not require element discretization in order to accurately capture the effects of material nonlinearity of a structural member, thus drastically reducing the degrees of freedom needed to model a structure. Such benefits have contributed to the popularity of the force based finite element method over displacement based finite element method when considering material nonlinearity of reinforced concrete structures. Zeris and Mahin (1988) have highlighted the numerical problems arising when using displacement based models. Mixed finite element method is a hybrid approach of force based and displacement based approaches. Spacone *et al*. (1996) have introduced a nonlinear beam finite element using mixed finite element approach. Recently, Saritas and Filippou (2013) have presented a mixed formulation based frame element, in cooperating axial-flexure-shear interaction using Timoshenko beam theory.

Force based finite element method was implemented in a line element by Menegotto and Pinto (1973) by interpolating both section deformations and section flexibilities to account axial force-bending moment interaction. Mahasuverachai and Powell (1982) introduced force dependent interpolation functions that are updated during the analysis. A force based fiber element was introduced by Kaba and Mahin (1984) and it was later improved by Zeris (1986), Zeris and Mahin (1988) and Zeris and Mahin (1991). The force based models proposed by Kaba and Mahin (1984), Zeris and Mahin (1988) and Zeris and Mahin (1991) failed to be integrated in to a general purpose finite element program due to the violation of initial equilibrium assumption. In addition, it was difficult to calculate element resisting forces corresponding to a given element nodal deformation. To overcome these problems, Ciampi and Carlesimo (1986) introduced a consistent force-based method which was later refined in Spacone *et al*. (1992) and Spacone *et al*. (1996a) to formulate force-based fiber beam-column element. Spacone *et al.* (1996b) applied this formulation to predict nonlinear hysteresis behavior of reinforced concrete beam specimen and proved that this element is accurate and numerically stable. Recent efforts were devoted to include effects of bond slip (Monti and Spacone (2000), Lobo and Almeida (2015)) and effects of large displacements (Souza (2000) and Sabry *et al*. (2018)) to the fiber beam column element. This element formulation is widely used by structural engineers all over the world including in structural analysis finite element packages such as OpenSees.

In the existing force-based fiber beam column element formulation, equilibrium, compatibility and constitutive relationships are satisfied at structure level, element level and fiber level respectively. It has two nested iterative procedures at structure level and element level. In the element level iterative procedure, the residual deformations at section level are integrated along an element to find element residual deformation. The calculated element residual deformation is minimized by applying an estimated element corrective force calculated by linearizing around the element stiffness of the previous iteration. This element level corrective force is distributed to all the sections of that element using force interpolation functions. Then section forces and deformations are updated to recalculate new section residual deformations. They are integrated again to find element residual deformation, which is compared with a tolerance value. This iterative procedure is followed until element residual deformation comes under a specified tolerance. Once the iteration has converged to the desired level of tolerance, the process yields element resisting forces for a given element deformation.

It is important to note that, the existing force-based fiber beam-column element formulation does not evaluate section level equilibrium directly. If a certain section behaves differently than others, the corrective force computed to reduce element level residual deformation may not be effective in addressing the problematic section, thus potentially resulting in an increased residual error in certain sections and reduced residual error in others. In this paper, a novel formulation is introduced, considering section level equilibrium at section level itself, through an iterative procedure. This allows the computation of section deformations and section stiffness that correspond to given section force increments, during section state determination itself.

The novel formulation can potentially act as a frame work to develop a finite element to predict nonlinear behavior of short columns, which has a massive impact on the holistic behavior of reinforced concrete frames as described in Caglar and Mutlu (2009). Feng *et al*. (2017) have formulated a displacement based fiber element to predict flexure-shear interaction. However, the prediction of flexure-shear interaction using force based finite element method is a difficult problem. The authors believe the proposed formulation enriches the existing force-based fiber beam-column element formulation, potentially opening doors towards addressing section specific phenomenon such as capturing the axial force-bending moment-shear force interaction that has proved difficult to capture through force based fiber element.

2. Model assumptions

The proposed flexibility based model is formulated for nonlinear static analysis of planar reinforced concrete structures, which exhibit material nonlinearity. The effects of geometric nonlinearity, bond slip and shear are not considered in the present study.

The proposed model utilizes four hierarchical levels namely, structure level, element level, section level and fiber level. It is based on force based finite element method with distributed plasticity having two nodes per element and each node having three degrees of freedoms. Accordingly, the element force vector and the deformation vector can be written as $\{P_1^* \; P_2^* \; P_3^* \; P_4^* \; P_5^* \; P_6^*\}^T$ and $\{U_1^* \; U_2^* \; U_3^* \; U_4^* \; U_5^* \; U_6^*\}^T$ respectively.

The aforementioned frame element can be expressed referring local coordinate system (x, y) through coordinate transformation. The element referring local coordinate system contains degrees of freedom that accounts for the motion resulting in both deformation of the element as well as rigid body translation and rotation. The rigid body modes has to be removed, so that the element flexibility matrix becomes invertible, allowing the computation of the element stiffness matrix. The state that contains only the degrees of freedom leading to the deformation of the element is referred as basic system and is shown in Fig. 1. The element force vector {Q} and element deformation vector {q} can written as shown in Eqs. (1)-(2).

$$\{Q\} = \{Q_1^e\ Q_2^e\ Q_3^e\}^T \tag{1}$$

$$\{q\} = \{q_1^e\ q_2^e\ q_3^e\}^T \tag{2}$$

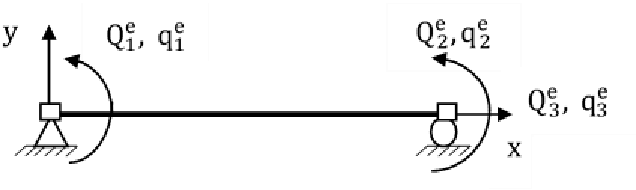

Fig. 1 Nodal forces and deformations of the basic system referring local coordinate system (x, y)

The proposed element monitors nonlinearity along the element at several control stations located at integration points. At each control station, a section is further subdivided in to several number of uniaxial fibers. Material stress strain relationship can be assigned to each concrete and steel fiber. Fig. 2 demonstrates the integration points and division of each section into fibers.

The proposed model is based on the assumption that plane section remains plane and perpendicular to the longitudinal axis. Accordingly, the section force vector can be expressed using axial force $N(x)$ and bending moment $M(x)$ while section deformation vector can be expressed using section curvature $\kappa(x)$ and axial strain at centroid axis $\varepsilon_0(x)$ as illustrated in Fig. 3. Therefore, section force and deformation vectors can be written as given in Eqs. (3)-(4).

$$\text{Section force} = \begin{Bmatrix} N(x) \\ M(x) \end{Bmatrix} \tag{3}$$

$$\text{Section deformation} = \begin{Bmatrix} \varepsilon_0(x) \\ \kappa(x) \end{Bmatrix} \tag{4}$$

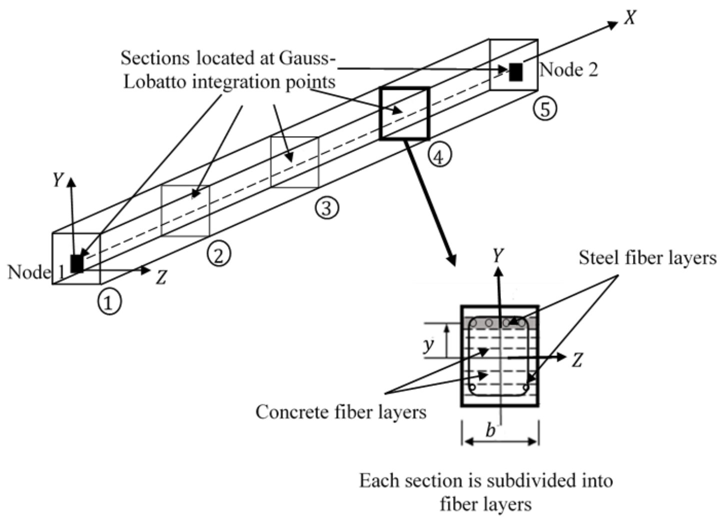

Fig. 2 The integration points and division of a section into fibers of the force based frame element without rigid body modes

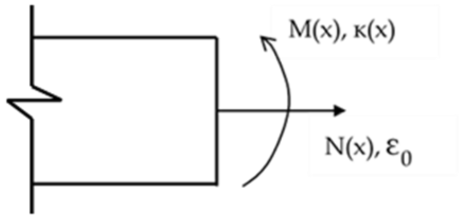

Fig. 3 Section forces and deformations at a control station

3. Proposed formulation

The proposed novel formulation is based on state determination processes at structure level, element level, section level and fiber level. There are two nested iterative procedures at structure level and section level. The formulation was written using displacement control method where displacement is applied in series of steps to a prescribed degree of freedom of the structure. By completing state determination processes at all hierarchical levels for a certain displacement step, structure force increment and deformation increment corresponding to the applied displacement step can be computed. By repeating this process for a series of displacement steps, the behaviour of the structure, element, section and fiber can be obtained. The state determination procedures are explained in the following section. Fig. 4 presents an overview of the proposed formulation.

3.1 Structure state determination

In displacement control method of structure state determination, an iterative procedure is used to calculate a force increment vector and a displacement increment vector corresponding to a certain displacement step U_2 at a specified degree of freedom. Initially, the incremental matrix equation of the structure is reduced by applying boundary conditions and it is rearranged such that rows and columns corresponding to degree of freedom where displacement step is applied is at the end. This allows to present the force increment vector, displacement increment vector and structure stiffness matrix in a condensed format. In the force increment vector, F_2 denotes the force increment value at the specified degree of freedom where displacement step is applied, F_1 denotes a vector of zeros as reaction components are left out by applying boundary conditions, P_1 denotes a zero vector and P_2 denotes unity and $\Delta\lambda$ represents the load factor. The structure force increment $\Delta\mathrm{F}$ in condensed format is given in Eq. (5).

$$\{\Delta \mathrm{F}\} = \begin{Bmatrix} \Delta \mathrm{F}_1 \\ \Delta \mathrm{F}_2 \end{Bmatrix} = \Delta\lambda \begin{Bmatrix} \mathrm{P}_1 \\ \mathrm{P}_2 \end{Bmatrix} \tag{5}$$

In the structure deformation increment vector, U_2 represents the displacement step applied and U_1 represent the displacement values of other degrees of freedom except the displacements at restrained degrees of freedom. The structure displacement increment $\Delta\mathrm{U}$ in condensed format is given in Eq. (6).

$$\{\Delta \mathrm{U}\} = \begin{Bmatrix} \Delta \mathrm{U}_1 \\ \Delta \mathrm{U}_2 \end{Bmatrix} \tag{6}$$

The condensed structure stiffness K is given in Eq. (7), where K_{22} represents a number, K_{12} a column vector, K_{21} a row vector and K_{11} a square matrix.

$$[\mathrm{K}] = \begin{bmatrix} \mathrm{K}_{11} & \mathrm{K}_{12} \\ \mathrm{K}_{21} & \mathrm{K}_{22} \end{bmatrix} \tag{7}$$

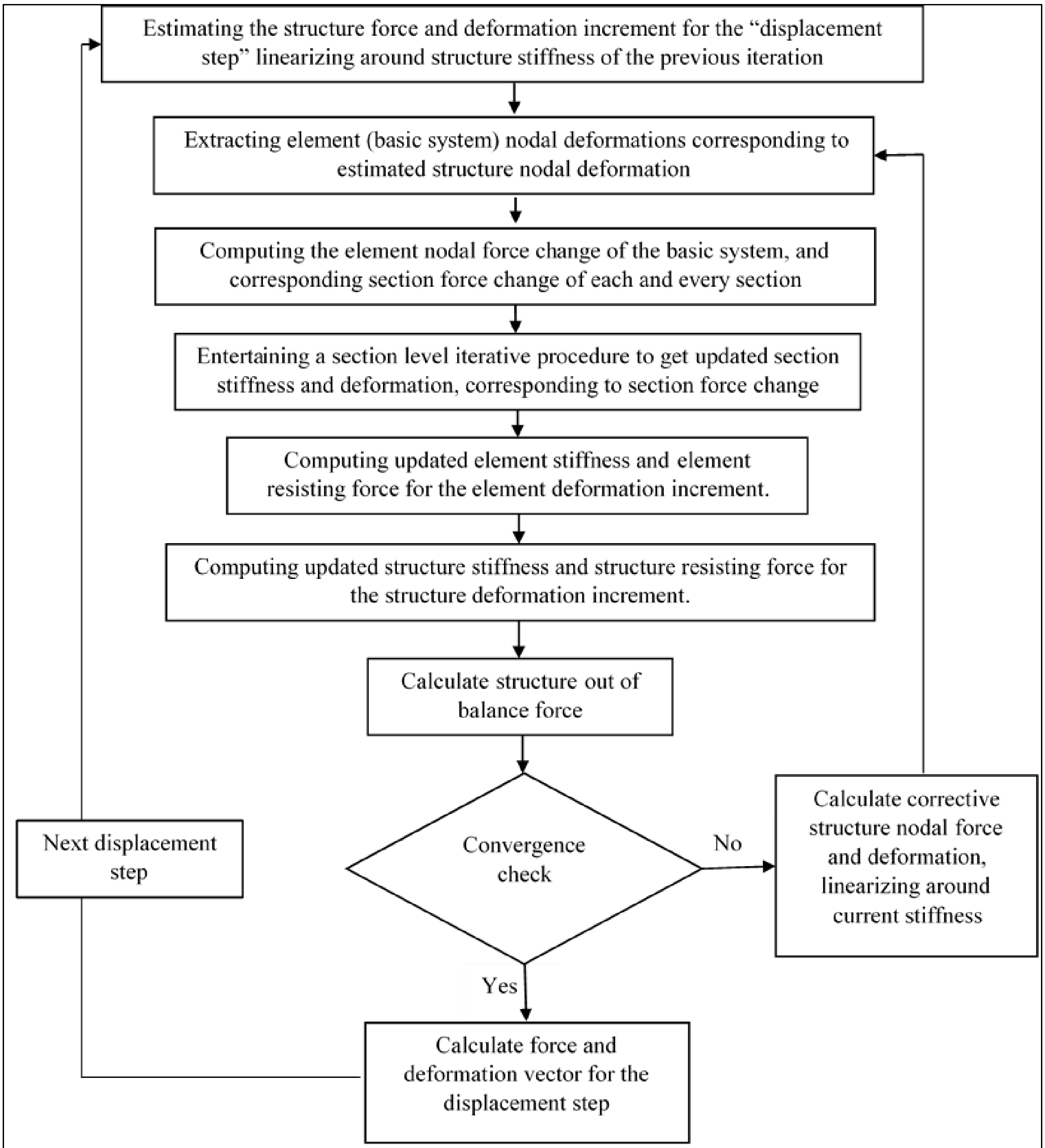

Fig. 4 Overview of the formulation

The rearranged structure stiffness matrix of the previous iteration is used to calculate an initial estimate of the force increment vector $\begin{Bmatrix} \Delta F_1 \\ \Delta F_2 \end{Bmatrix}^{i=1}$ and displacement increment vector $\begin{Bmatrix} \Delta U_1 \\ \Delta U_2 \end{Bmatrix}^{i=1}$, which corresponds to the applied displacement step at the specified degree of freedom as shown in Eq. (8).

Here, i denotes the structure level iteration number.

$$\Delta\lambda^{i=1}\begin{Bmatrix}P_1\\P_2\end{Bmatrix} = \begin{bmatrix}K_{11} & K_{12}\\K_{21} & K_{22}\end{bmatrix}_{i=0}\begin{Bmatrix}\Delta U_1\\\Delta U_2\end{Bmatrix}^{i=1} \quad (8)$$

Then the structure resisting force $\begin{Bmatrix}R_1\\R_2\end{Bmatrix}^{i=1}$ corresponding to the estimated structure deformation increment can be calculated using the updated structure stiffness matrix generated by delving to element level and section level. This computation is shown in Eq. (9). R_2 represents the resisting force at the degree of freedom where the displacement step is applied while R_1 denotes resisting force vector of other degrees of freedom excluding the values at restrained degrees of freedom. The updated structure stiffness matrix is generated by assembling section stiffness resulted from an iterative procedure at the section level which will be discussed later.

$$\begin{Bmatrix}R_1\\R_2\end{Bmatrix}^{i=1} = \begin{bmatrix}K_{11} & K_{12}\\K_{21} & K_{22}\end{bmatrix}_{i=1}\Delta\begin{Bmatrix}U_1\\U_2\end{Bmatrix}^{i=1} \quad (9)$$

The out of balance forces $\begin{Bmatrix}O_1\\O_2\end{Bmatrix}^{i=1}$ can be then calculated as given in Eq. (10). O_2 represents the out of balance force at the degree of freedom where the displacement step is applied, while O_1 denotes out of balance force vector of other degrees of freedom excluding the values at the restrained degrees of freedom.

$$\begin{Bmatrix}O_1\\O_2\end{Bmatrix}^{i=1} = \Delta\lambda^{i=1}\begin{Bmatrix}P_1\\P_2\end{Bmatrix} - \begin{Bmatrix}R_1\\R_2\end{Bmatrix}^{i=1} \quad (10)$$

If the out of balance force is not within the tolerance, a suitable corrective force factor ($\Delta\lambda^{i=2}$) and a deformation increment $\begin{Bmatrix}\Delta U_1\\\Delta U_2\end{Bmatrix}^{i=2}$ are calculated to neutralize this out of balance force, keeping the displacement of the specified degree of freedom constant and using the updated structure stiffness matrix as given in Eq. (11) where i represents the structure level iteration number.

$$\begin{Bmatrix}\Delta U_1\\\Delta U_2\end{Bmatrix}^{i=2} = \begin{bmatrix}K_{11} & K_{12}\\K_{21} & K_{22}\end{bmatrix}_{i=1}^{-1}\begin{Bmatrix}O_1\\O_2\end{Bmatrix}^{i=1} + \begin{bmatrix}K_{11} & K_{12}\\K_{21} & K_{22}\end{bmatrix}_{i=1}^{-1}\Delta\lambda^{i=2}\begin{Bmatrix}P_1\\P_2\end{Bmatrix} \quad (11)$$

At this point the load factor and structure deformation vector can be updated as given in Eqs. (12)-(13).

$$\lambda = \lambda + \Delta\lambda^{i} \quad (12)$$

$$U = U + \begin{Bmatrix}\Delta U_1\\\Delta U_2\end{Bmatrix}^{i} \quad (13)$$

At the start of the next iteration, resisting force corresponding to the previous corrective structure deformation needs to be calculated. For this purpose, updated structure stiffness matrix corresponding to the new structure force increment or correction is calculated as before by an iterative procedure at section level (section state determination). Resisting force calculation at a general iteration i is given in Eq. (14).

$$\begin{Bmatrix}R_1\\R_2\end{Bmatrix}^{i} = \begin{bmatrix}K_{11} & K_{12}\\K_{21} & K_{22}\end{bmatrix}_{i}\begin{Bmatrix}\Delta U_1\\\Delta U_2\end{Bmatrix}^{i} \quad (14)$$

At a general iteration i, out of balance force is calculated by Eq. (15).

$$\begin{Bmatrix}O_1\\O_2\end{Bmatrix}^{i} = \begin{Bmatrix}O_1\\O_2\end{Bmatrix}^{i-1} + \Delta\lambda^{i-1}\begin{Bmatrix}P_1\\P_2\end{Bmatrix} - \begin{Bmatrix}R_1\\R_2\end{Bmatrix}^{i} \quad (15)$$

If the out of balance force is still outside the tolerance, the structure deformation and force are corrected again by Eq. (11). This procedure is continued until the out of balance force comes inside a prescribed tolerance. Fig. 5 shows a schematic diagram of structure state determination. Point A represents the converged force and deformation vectors of the previous displacement step. If the out of balance forces generated after fourth structure level iteration $O^{i=4}$ is sufficiently small, point B represents the correct force and deformation vectors corresponding to the current displacement step.

3.2 Element state determination

At the first structure level iteration of a certain displacement step, the structure force increment and displacement increment corresponding to a displacement at a specified degree of freedom is estimated as given in Eq. (8). At the beginning of element state determination, element nodal deformation increments referring global coordinate system $\{\Delta q^{e}_{global,i}\}$ is extracted from the structure deformation increment ($when\ i = 1$) or the corrective structure deformation increment $(when\ i > 1)$ $\Delta U_{stiffness\ cal,i}$. These element nodal deformations are then expressed referring local coordinate system by multiplying with the rotational transformation matrix $\{r_{ROT}\}$ as shown in Eq. (16). Here the superscript e denotes the element.

$$\{\Delta q^{e}_{local,i}\} = [r_{ROT}]\{\Delta q^{e}_{global,i}\} \tag{16}$$

Rigid body modes are then removed using rigid body transformation matrix $[r_{RBM}]$ to obtain element nodal deformations of the basic system $\{\Delta q^{e}_{i}\}$ as shown in Eq. (17). Then the element deformation vector $\{q^{e}\}$ can be updated as in Eq. (18)

$$\{\Delta q^{e}_{i}\} = [r_{RBM}]\{\Delta q^{e}_{local,i}\} \tag{17}$$

$$\{q^{e}\} = \{q^{e}\} + \{\Delta q^{e}_{i}\} \tag{18}$$

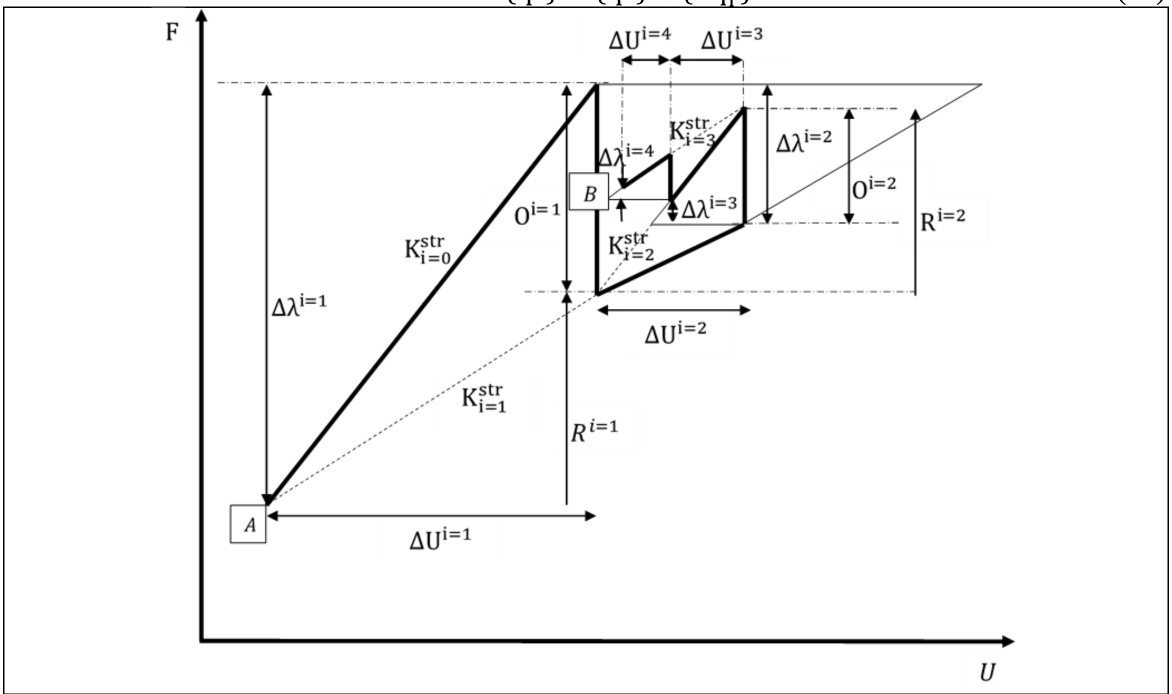

Fig. 5 Schematic diagram of structure state determination

The stiffness matrix of the previous iteration, together with Δq_i^e will yield the force increment ($when\, i = 1$) or correction ($when\, i > 1$) of the basic system, corresponding to force and deformation correction at structure level as shown in Eq. (19). The element unbalanced force $\Delta Q^{e}_{unb,i-1}$should be omitted from the equation in the first structure level iteration. The computation of $Q^{e}_{unb,i-1}$ is done using the updated element stiffness matrix as shown in Eq. (26). Accordingly element force vector (Q^e) can be updated as shown in Eq. (20)

$$\{\Delta Q^{e}_{i}\} = [K_{i-1}]\{\Delta q^{e}_{i}\} - \{Q^{e}_{unb,i-1}\} \tag{19}$$

$$\{Q^{e}\} = \{Q^{e}\} + \{\Delta Q^{e}_{i}\} \tag{20}$$

At this point, section force increments $\{\Delta S^{h}_{i}\}$ and section forces $\{S^{h}_{i}\}$ of each section of the element can be calculated using force interpolation function $[N^{h}]$ which corresponds to each section as shown in Eqs. (21)- (22). Here, the superscript h denotes the section.

$$\{\Delta S^{h}_{i}\} = [N^{h}]\{\Delta Q^{e}_{i}\} \tag{21}$$

$$\{S^{h}_{i}\} = \{S^{h}_{i}\} + \{\Delta S^{h}_{i}\} \tag{22}$$

Subsequently, a process called section state determination is done for all the sections to find updated section stiffness and section deformations of all the sections of the element corresponding to section force increment at each section. By assembling the updated section stiffness, updated element stiffness matrix can be obtained as given in Eq. (23). Here f^{s}_{h} denotes section flexibility matrix.

$$[f_e] = \int_{0}^{L} [N^{h}(x)]^{T}[f^{s}_{h}][N^{h}(x)]dx \cong \sum_{1}^{nIP} [N^{h}]^{T}[f^{s}_{h}][N^{h}] \tag{23}$$

The updated element flexibility matrix $[f_e]$ can be inverted to find the element stiffness of the basic system as shown in Eq. (24).

$$[k^{e}] = [f^{e}]^{-1} \tag{24}$$

The updated element stiffness matrix is used to compute element resisting force corresponding to the element deformation increment (when $i = 1$) or corrective deformation increment (when $i > 1$) as shown in Eq. (25). The element unbalanced force vector is computed by Eq. (26).

$$\{Q^{e}_{res,i}\} = [K^{e}_{i}]\{\Delta q^{e}_{i}\} \tag{25}$$

$$\{Q^{e}_{unb,i}\} = [K_{i-1}]\{\Delta q^{e}_{i}\} - \{Q^{e}_{res}\} \tag{26}$$

Subsequently, by introducing rigid body modes and writing it with reference to global coordinate system, element stiffness matrix referring global coordinate system can be obtained as shown in Eq. (27).

$$[K^{e}] = [\tau_{ROT}]^{T}([\tau_{RBM}]^{T}[k^{e}][\tau_{RBM}])\,[\tau_{ROT}] \tag{27}$$

By assembling the updated element stiffness matrices of all the elements, updated structure stiffness matrix corresponding to the structure force increment vector or the correction can be computed. The element unbalanced force vector $\{Q^{e}_{unb,i}\}$ calculated in Eq. (26) is not corrected at element level, instead structure resisting force vector is computed and structure unbalance force vector is minimized entertaining the iterative procedure mentioned at structure state determination. The corrective forces and deformations decided at the structure level are applied at the element level to get the updated element force and deformation vectors. Therefore, within each Newton-Raphson iteration, element nodal force and deformation vectors are updated. By the completion of all state determination procedures for one displacement step, the unbalanced forces at the element level will be automatically minimized. A summary of element state determination procedure is given in Fig.

6. Fig. 7 illustrates the element state determination procedure. It is important to note that no iteration occurs at this level. Subscript i represents the iteration number at the structure level.

3.3 Section state determination

Section state determination is designed to generate the section stiffness matrix and deformation vector which satisfy section level equilibrium with the section force increment calculated in Eq. (21). Using the section stiffness matrix of the previous iteration, an initial estimate of the section deformation increment vector $\{\Delta e_z^h\}$ is calculated as given in Eq. (28). Subsequently the section deformation is updated as in Eq. (29). The subscript z denotes the iteration number at the section level.

$$\{\Delta e_z^h\} = [K_{sec,z-1}^{-1}]\{\Delta S_i^h\} \tag{28}$$

$$\{e^h\} = \{e^h\} + \{\Delta e_z^h\} \tag{29}$$

The section resisting force vector $\{\Delta S_{res}^h\}$ and the stiffness $[K_{sec,z}]$ corresponding to the section deformation vector $\{e^h\}$ can be then calculated by delving to fiber level. Afterwards, the section unbalanced force vector $\{\Delta S_{unb}^h\}$ can be calculated by the difference between the section force vector and resisting force vector as given in Eq. (30)

$$\{\Delta S_{unb,z}^h\} = \{S_i^h\} - \{S_{res,z}^h\} \tag{30}$$

If the section unbalanced force vector is not small enough, a corrective section deformation increment is applied based on the unbalanced force and the updated tangent section stiffness. Then the section deformation vector is updated again by adding the corrective deformation. Subsequently, the section resisting force vector and the section stiffness matrix corresponding to the updated section deformation vector can be computed, which can be utilized to calculate any remaining unbalanced force. By going through several iterative steps, section unbalanced force can be minimized.

It is important to note that this minimization of section unbalanced forces implies that the section has reached an equilibrium configuration which corresponds to the force increment vector of the section $\{\Delta S_i^h\}$. Once the equilibrium state is achieved, it yields correct section deformation and stiffness for the section force increment $\{\Delta S_i^h\}$.

Fig. 8 illustrates the section level iterative procedure graphically and Fig. 9 illustrates the section level iterative procedure with the aid of flow chart. In Fig. 8, point A represents the converged section forces and deformations at the end of $(i-1)^{th}$ structure level iteration. If the section unbalanced forces generated at the end of third section level iteration is small enough, the point B represents the converged section forces and deformations of the i^{th}structure level iteration.

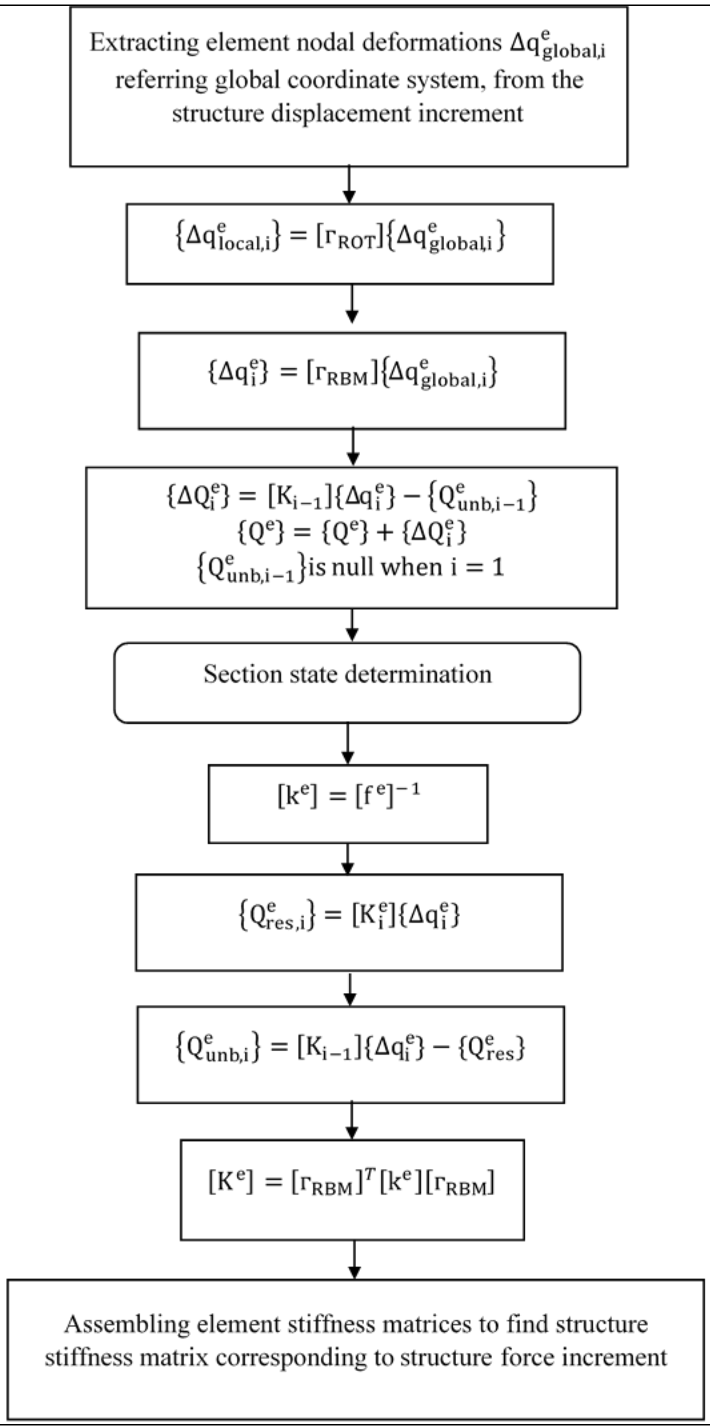

Fig. 6 Flow chart of element state determination

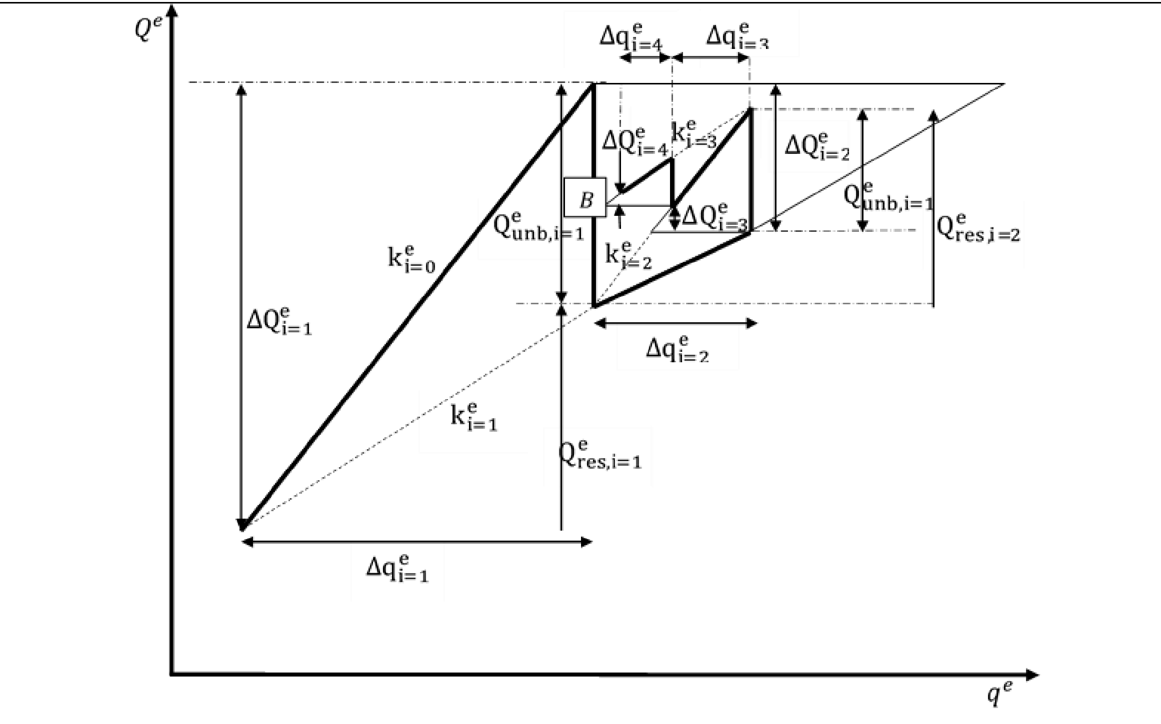

Fig. 7 Schematic diagram of element state determination

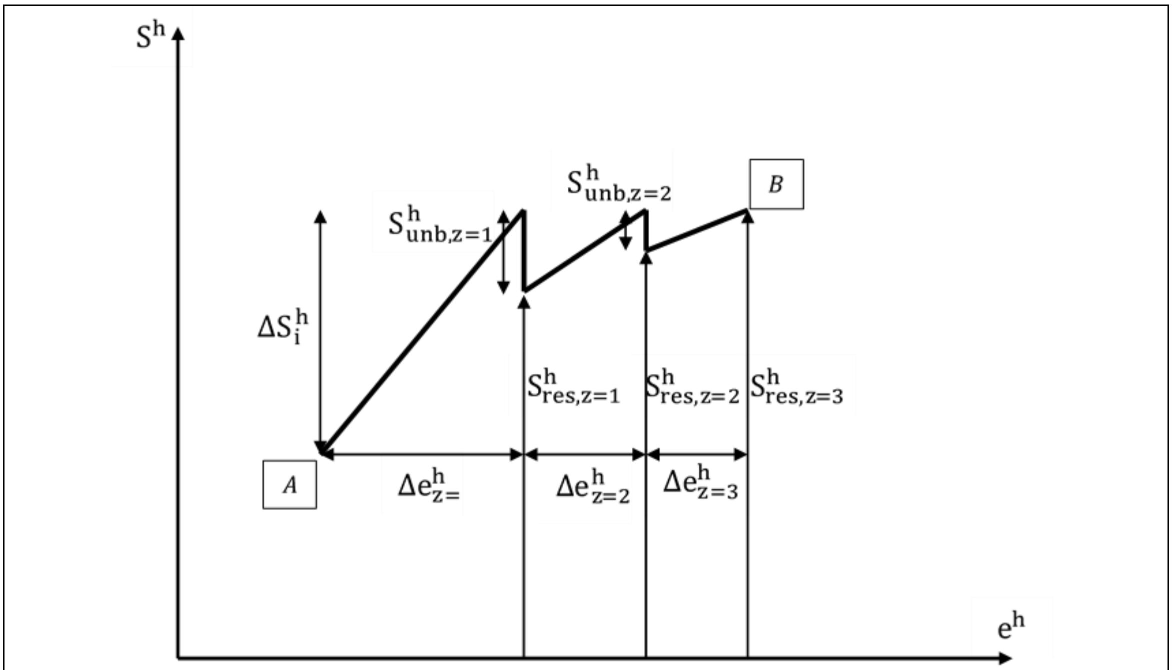

Fig. 8 Schematic representation of section state determination

3.4 Fiber state determination

The fiber state determination process is designed to calculate the section resisting force and updated section stiffness corresponding to a given section deformation. The sections at control stations are divided in to a sufficient number of uniaxial fibers. With the assumption that the plane section remains plane and perpendicular to the longitudinal axis, strains of each fiber can be calculated using the given section deformation vector as given in Eq. (31)

$$\varepsilon_{fib} = \{1 \quad -y_{fib}\}\begin{Bmatrix} \varepsilon_0 \\ \kappa(x) \end{Bmatrix} \tag{31}$$

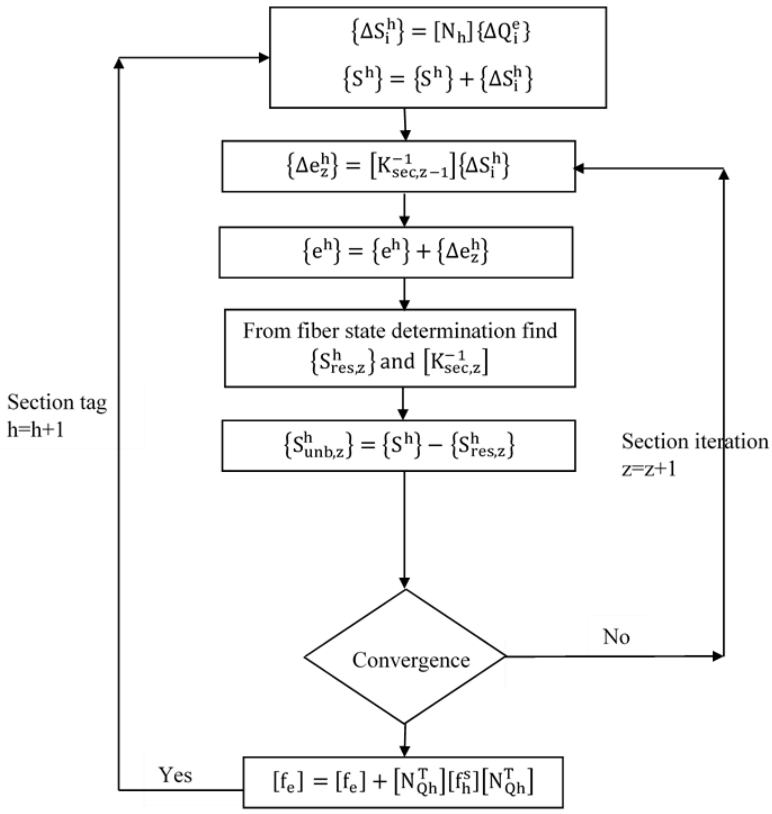

Fig. 9 Flow chart of section state determination

From the material model assigned to each fiber, fiber stress σ_{fib} and fiber tangent stiffness $E_{T,fib}$ corresponding to fiber strains can be obtained. Based on the fiber section model, section resisting forces can be calculated using Eq. (32) and the section stiffness can be calculated using Eq. (33).

Here, A_{fib} denotes the fiber area.

$$S^{h}_{res,z} = \sum_{nof=1}^{Nof(x)} \begin{Bmatrix} 1 \\ -y \end{Bmatrix} \sigma_{fib} A_{fib} \tag{32}$$

$$K_{sec} = \sum_{nof=1}^{Nof(x)} \begin{Bmatrix} 1 \\ -y \end{Bmatrix} E_{T,fib} A_{fib} \{1 \quad -y\} \tag{33}$$

The accuracy of the Eqs. (32)- (33) depends on the number of fibers used and there locations. If the number of fibers are too small the capacity of the section will be under estimated. If the number of fibers are too high the calculation will be computationally expensive. .

3.5 Indirect satisfaction of compatibility

The novel formulation satisfies the law of constitutive relationship at the fiber level, while equilibrium is evaluated at both the structure level and the section level. However, it should be noted that the compatibility relationship is satisfied indirectly.

The iterative procedure at the section level is designed to generate correct section deformation and correct stiffness for a given section force increment. The generated section deformation and section stiffness perfectly match with section force increment. Therefore, the compatibility relationship at the section level is automatically satisfied. At the structure level and the element level resisting forces are calculated using the correctly updated stiffness matrix generated from section level iterative procedure. In addition, corrective deformations and corrective forces at structure level are computed using the correctly updated structure stiffness matrix. Hence the law of compatibility is satisfied indirectly in the proposed formulation.

4. Experimental validation

The proposed model was validated against experimental response and OpenSees response of a flexural cantilever wall RW2 (Thomsen and Wallace (1995)). Then a two dimensional single storey frame was analyzed using the proposed formulation and OpenSees software to compare load – deformation responses. The model in Popovics (1973) and bilinear model were used as concrete and steel material constitutive relationships.

4.1 Flexural cantilever wall

The reinforced concrete cantilever wall RW2 was experimented by Thomsen and Wallace (1995). The wall was designed to behave in a flexure dominant manner. Table 1 demonstrates the details of RW2 while Fig. 10 illustrates the loading arrangement and the reinforcement details of the cross section.

Table 1 Details of RW2

Height (mm)	3660
Outer perimeter Depth x width (mm x mm)	1220 x 102
Aspect ratio (l/d)	3
Compressive axial load (kN)	240.41
Cube strength (MPa)	42.8
Yield strength of longitudinal reinforcement (MPa)	414

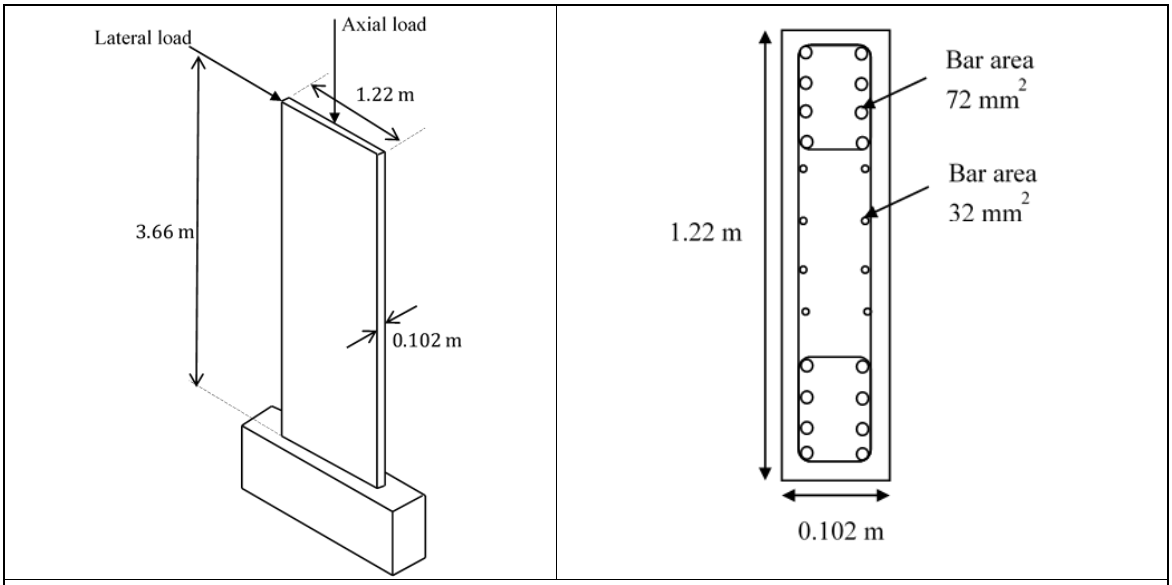

Fig. 10 Loading arrangement, dimensions and reinforcement details of RW2

The numerical inputs used in the proposed model and OpenSees software are tabulated in Table 2. Fig. 11 brings forward the load- deformation response comparison of the flexure dominant cantilever wall RW2, using the proposed formulation, OpenSees and experimental response. It is important to note that OpenSees software has the nonlinear force based fiber beam column element, or in other words existing formulation to predict axial force- bending moment interaction of RC structures. The load- deformation responses in the three cases are in very good agreement. The nonlinear behaviors such as tensile concrete cracking, tensile steel yielding and ductile behavior were very well captured by the proposed model.

The first concrete tensile crack occurs around 10 kN load. The propagation of concrete tensile cracking causes a significant reduction of the slope in the load deformation curve around 30 kN load. The tensile cracking of concrete shifts the centroid axis towards the compression zone.

Table 2 Numerical inputs used in the analytical models

Input Parameter	**Novel formulation**	**OpenSees model**
Number of elements	1	1
Number of integration points	6	6
Number of fibers	20	20
Section level force tolerance (kN or kNm)	10^{-10}	-
Element level residual deformation tolerance (m)	-	10^{-8}
Structure level force tolerance (kN or kNm)	10^{-5}	10^{-5}

Once the concrete tensile cracking stagnates, the slope of load-deformation curve becomes approximately constant until 98 kN where tensile steel yielding initiates. However, a slight reduction of concrete tangent stiffness is reflected by the slight reduction of the slope in the load- deformation response. The structure stiffness drops drastically with the tensile steel yielding and remains constant producing a ductile behavior. The stress and strain distributions of all the sections at different stages of the load-deformation response are given in Figs. 12- 15. The section numbers correspond to Gauss-Lobatto integration point number, where section 1 corresponds to the one at the fixed support. It should be noted that the proposed model was able to predict the complete experimental load-deformation response, while the OpenSees model with the specified parameters was able to predict the half way of the full load-deformation response as illustrated in Fig. 11.

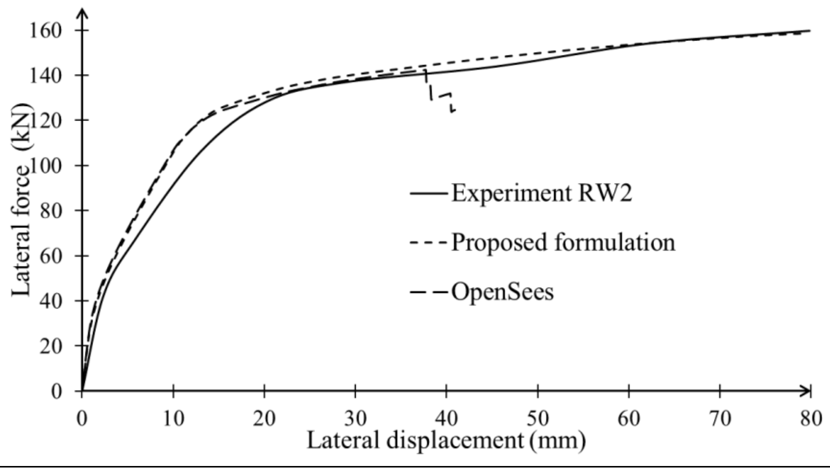

Fig. 11 Load deformation responses of the RW2 cantilever wall obtained experimentally, using novel formulation and using OpenSees software

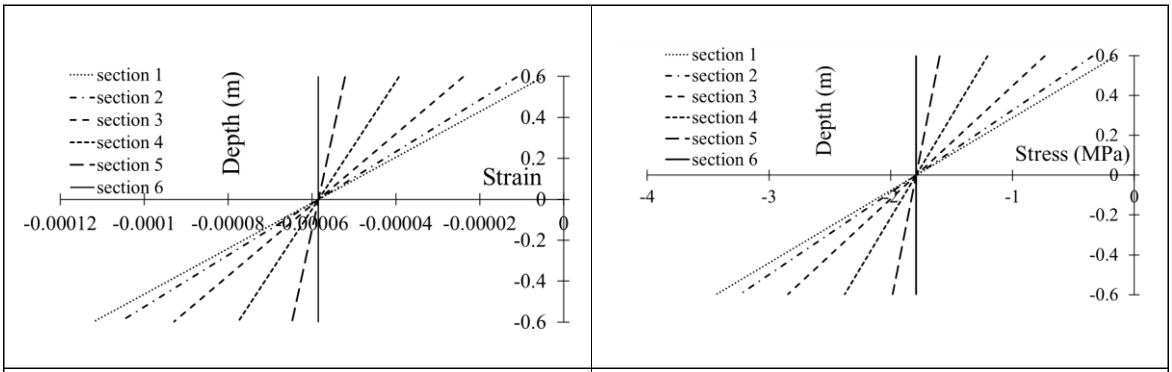

(a) Strain variation of sections with depth

(b) Stress variation of sections with depth

Fig. 12 At 10 kN load

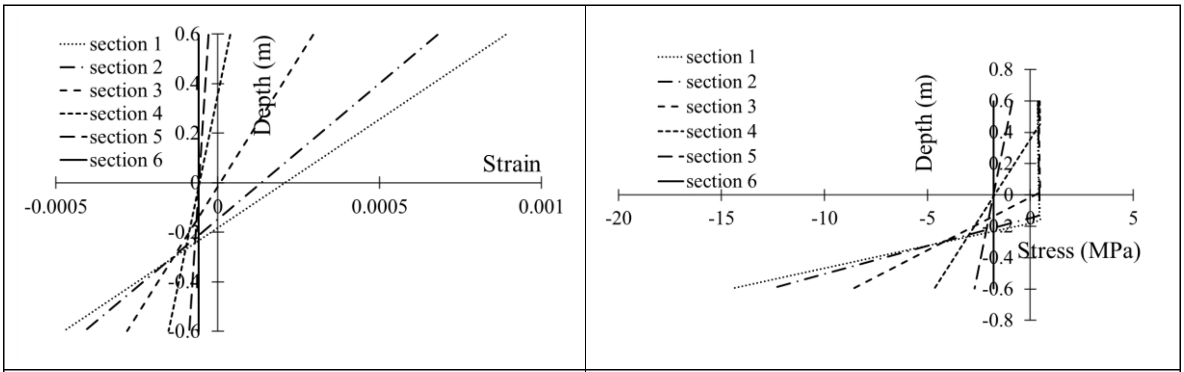

(a) Strain variation of sections with depth

(b) Stress variation of sections with depth

Fig. 13 At 63 kN load

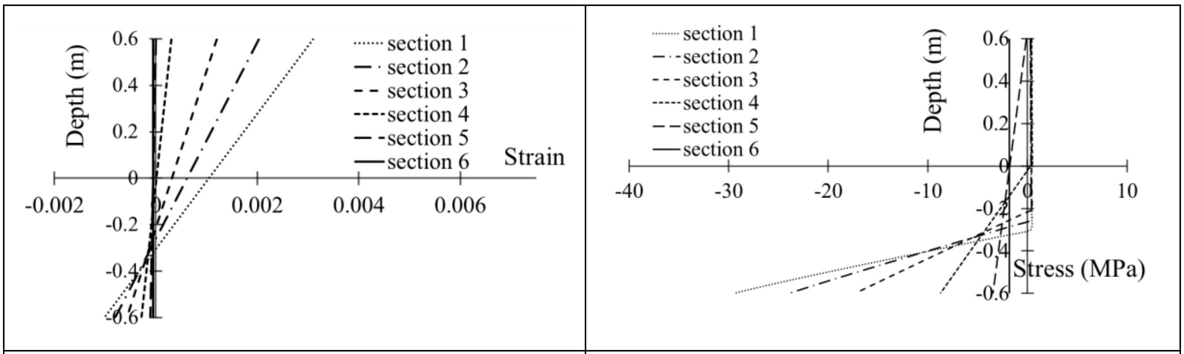

(a) Strain variation of sections with depth

(b) Stress variation of sections with depth

Fig. 14 At 115 kN load

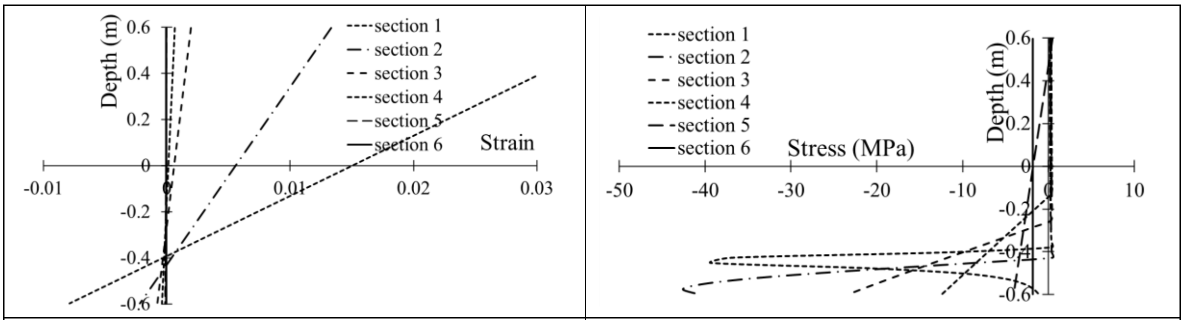

(a) Strain variation of sections with depth

(b) Stress variation of sections with depth

Fig. 15 At 154 kN load

4.2 Single storey two dimensional frame

The response of a single storey plane frame predicted by the proposed model is compared with the response obtained from OpenSees software to test the accuracy and the stability of the proposed model in predicting nonlinear response.
The dimensions, loading arrangement, cross section and reinforcement details of the planar reinforced concrete single storey frame is given in Fig. 16. The numerical inputs used in the two simulations are tabulated in Table 3.

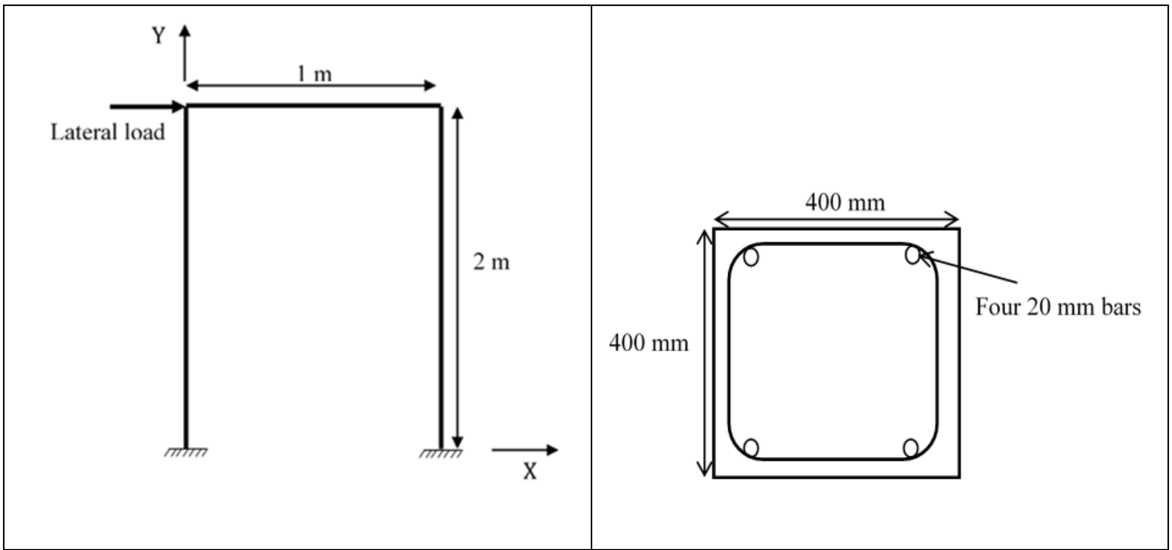

Fig. 16 The dimensions, loading arrangement and reinforcement details of all beams and columns of the planar reinforced concrete single storey frame.

Figure 17 presents the comparison of the load deformation responses of the single storey frame, using the novel formulation and OpenSees. Both the proposed formulation and OpenSees were able to capture the concrete tensile cracking and tensile steel yielding behaviors identically. The graphs depicts a very good agreement, thus the proposed formulation is verified with the OpenSees software.

Table 3 Numerical inputs used in proposed model and OpenSees model

Input Parameter	**Novel formulation**	**OpenSees model**
Number of elements	3	3
Number of integration points	6	6
Number of fibers	20	20
Section level force tolerance (kN or kNm)	10^{-10}	-
Element level residual deformation tolerance (m)	-	10^{-8}
Structure level force tolerance (kN or kNm)	10^{-5}	10^{-5}

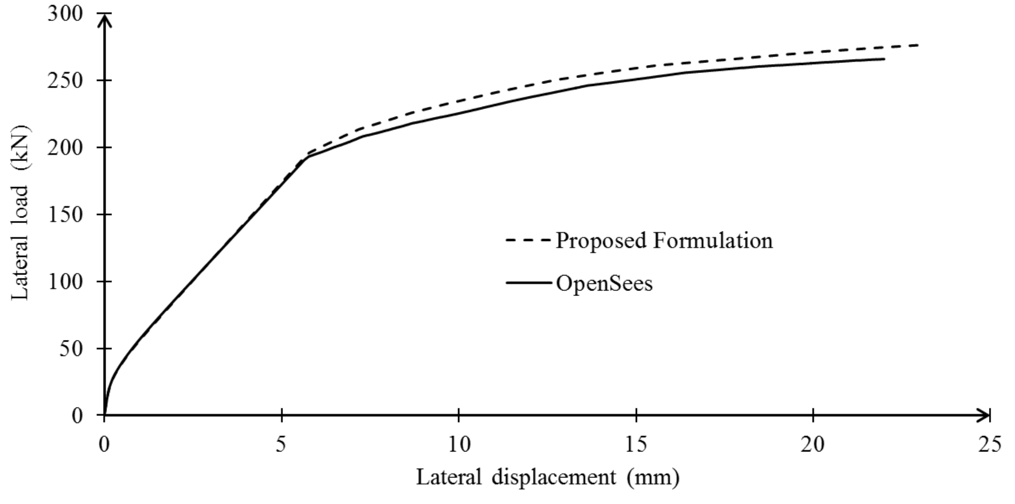

Fig. 17 Load – deformation response of planar reinforced concrete single storey frame using OpenSees and proposed formulation

6. Potential advantages of considering section level equilibrium

6.1 Control of force tolerance at section level

The proposed formulation directly evaluate the agreement between section force and section deformation by reducing the unbalanced force between section force and section resisting force. The tolerance value used in the section level iterative procedure is under the control of the user. Therefore, the proposed formulation allows the user of this model to decide the required accuracy at the section level. However, the existing formulation does not directly minimize the residual deformations at section level. Instead, it entertains an iterative procedure at element level to minimize element residual deformations which are computed by integrating section residual deformations. Therefore, the existing formulation does not facilitate to control force tolerance at section level. The control of accuracy at section level, allows the users to prescribe optimum tolerance values to get accurate solutions with minimum computational cost.

The moment – curvature relationships at integration points of the reinforced cantilever wall RW2, were drawn for the responses from the OpenSees software and the proposed formulation. Fig. 23 demonstrates that there is a significant difference in the moment curvature relationships in the two models. The section 1 refers to the Gauss-Lobatto integration point at the fixed support. It is important to note that in this example, the proposed formulation has checked the agreement between section force and deformation for a force tolerance of 10^{-10} (kN or kNm) while the existing formulation have minimized the residual deformations at element level to a displacement accuracy of 10^{-8} (m or rad).

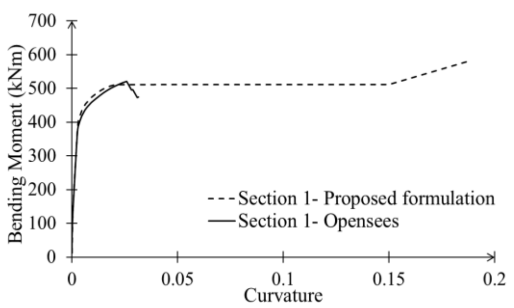

(a) Section 1

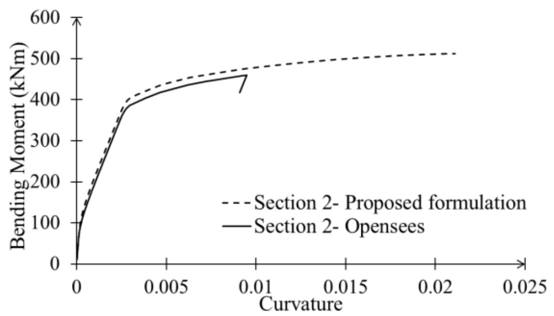

(b) Section 2

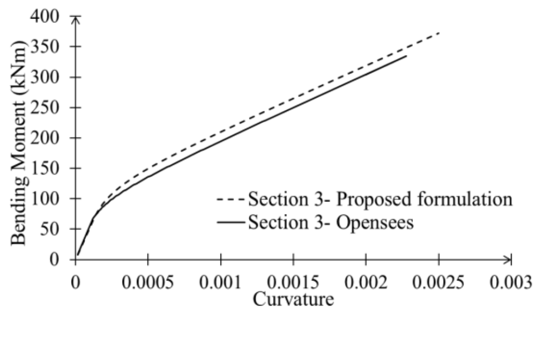

(c) Section 3

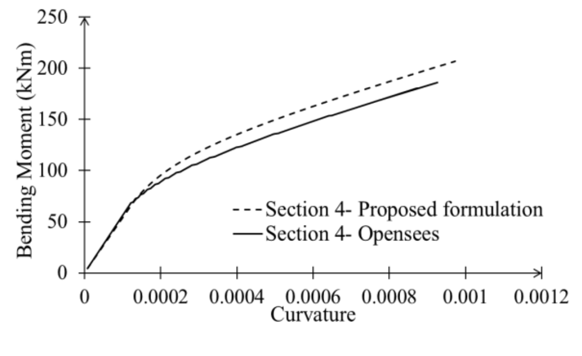

(d) Section 4

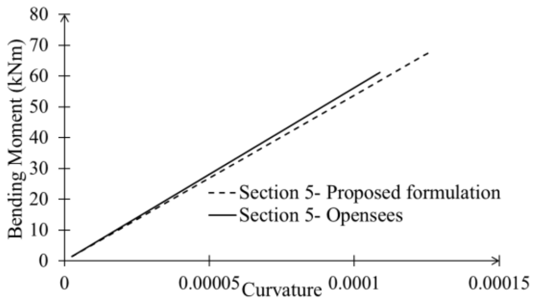

(e) Section 5

Fig. 18 Bending moment-curvature response of RW2, using proposed formulation and Opensees.

It is also important to note that, displacement values are inherently small and it is notoriously difficult to predict an accuracy level using a deformation value, thus considering section level equilibrium allows the user to decide a section level tolerance value in a practical sense.

6.2 Effective Newton – Raphson procedure at structure level

At structure level, in both the existing and proposed element formulations, Newton Raphson procedure is implemented to find structure nodal deformation for an applied force step. Within a single iterative step, structure nodal deformation increment corresponding to unbalanced force is estimated and corresponding resisting force and unbalanced force is evaluated. The two formulations differ from the way in which structure resisting forces are calculated.

In the existing fiber beam column element formulation, the element level iterative procedure is designed to find element resisting forces for the estimated element nodal deformations by minimizing element residual deformations. It should be noted that the section residual deformations due to complex section specific behaviors such as concrete cracking, tensile steel yielding are corrected by the aforementioned procedure at element level by minimizing element residual deformations. Therefore, within a certain Newton Raphson iterative step, the equilibrium of the elements are yet to be checked even though the element resisting forces are found for a given nodal deformations. According to these facts, in the existing element formulation, Newton Raphson procedure is assigned with the additional task of satisfying equilibrium at element level and section level.

The section level iterative procedure introduced in the proposed formulation allows to calculate section stiffness matrix and section deformation vector for a given section force increment, satisfying equilibrium at section level itself. Within a Newton Raphson iteration, equilibrium is satisfied at section level for the given section force increments and assembled updated structure stiffness matrix is used to calculate structure resisting force corresponding to the structure nodal deformation estimation. The Newton Raphson procedure is utilized only to adjust the structure nodal deformations, and section forces such that the unbalanced force at structure level is minimized. Extra effort is not required to obtain equilibrium at element level and section level. Therefore, the Newton Raphson procedure is effective in the proposed formulation.

In order to support this argument, the cantilever reinforced concrete wall, RW2 was analyzed restricting newton Raphson iterations to one. Fig. 26 provides a comparison of the load-deformation responses where a very good agreement could be seen. This reflects the effectiveness of the Newton Raphson process in the proposed formulation. Please note that the analysis was done using displacement control method.

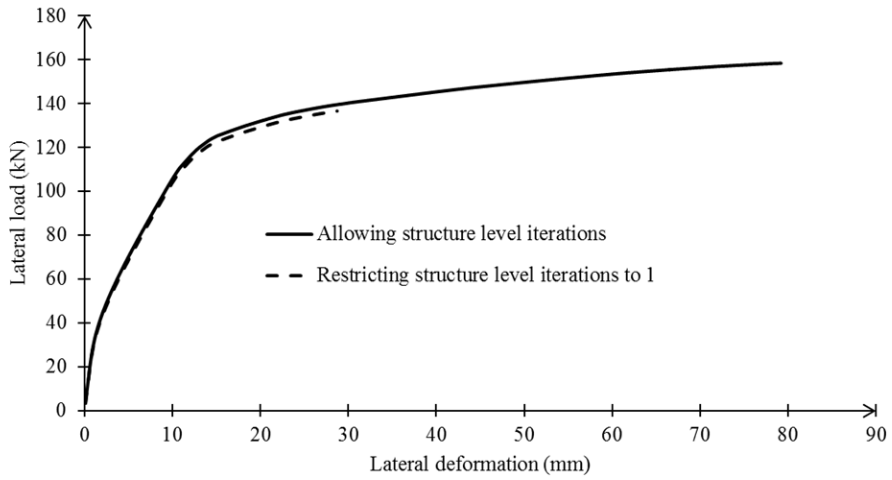

Fig. 19 Load deformation responses of RW2, allowing and restricting structure level iterations using the proposed formulation

It is also important to note that when the structure is statically determinate and analysis is done using force control method, one Newton Raphson iteration will generate the correct structure deformation. This could be explained by the fact that section force increments perfectly matches the applied structure force in the case of statically determinate structures. If the section force increments are correct, the updated section stiffness will generate correct structure stiffness which can be used to calculate correct structure nodal deformation using one Newton-Raphson iteration.

The structure level and section level iterative procedures reduce structure unbalanced force and update section stiffness matrices for a given force increment. However, there is no direct iterative procedure to reduce unbalance force at the element level. Once the element resisting forces and unbalanced forces are computed using updated element stiffness matrices, they are corrected at structure level and the corresponding corrective deformation is applied to each element. Thus the element force and deformation vectors are updated within each Newton-Raphson iteration, even though there is no separate iterative procedure for the element level. By completion of the whole process for a displacement step, the element unbalanced forces and residual deformations are minimized in order to have correct element force displacement relationship. Therefore, shifting the iterative procedure to section level will not compromise the equilibrium of element level.

7. Conclusions

This paper presents a novel force based finite element formulation to predict axial force – bending moment interaction considering section level equilibrium. The existing formulation proposed by Spacone *et al*. (1996a) satisfies the laws of equilibrium, compatibility and constitutive relationship at structure level, element level and fiber level with the aid of two nested iterative procedures at structure level and element level. However, it does not facilitate to evaluate section level equilibrium. The proposed formulation entertains two nested iterative procedures at section level and structure level where equilibrium is satisfied. The constitutive law is satisfied at fiber level while the law of compatibility is satisfied by the computation of correct section deformation and correct stiffness for a given section force at section level. The proposed formulation was validated with a reinforced cantilever wall, RW2 experimented by Thomsen and Wallace (1995). Subsequently, the response of the proposed formulation was verified with Opensees software using a single storey two dimensional frame. The proposed formulation proved to be accurate and numerically stable to predict axial force – bending moment interaction of reinforced concrete frames and walls. Finally, the potential advantages of considering section level equilibrium were highlighted. The authors believe the proposed formulation enriches the existing force – based fiber beam column element formulation, potentially opening doors towards addressing section specific phenomenon such as capturing the axial force-bending moment-shear force interaction that has proved difficult to capture.

Acknowledgments

The research described in this paper was financially supported by the Department of Civil Engineering, University of Peradeniya, Sri Lanka.

References

Caglar, N. and Mutlu, M. (2009), “Failure analysis of reinforced concrete frames with short column effect”, *Computers and Concrete*, **6**(5), 403-419.

Ciampi, V. and Carlesimo, L. (1986), “A nonlinear beam element for seismic analysis of structures”, *Proceedings of the 8th European Conference on Earthquake Engineering*, Lisbon, Portugal.

Colangelo, F. (2018), “Effect of axial force-bending moment interaction of stochastic nonzero mean seismic response of reinforced concrete frames”, *Engineering Structures*, **174**, 139-153.

Feng, D., Wu, G., Sun, Z. and Xu, J. (2017), “A flexure-shear Timoshenko fiber beam element based on softened damage-plasticity model”, Engineering Structures, **140**, 483-497.

IU, C.K. (2016), “Nonlinear analysis of the RC structures by higher-order element with the refined plastic hinge”, *Computers and Concrete*, **17**(5), 579-596.

Kaba, S. and Mahin, S. A. (1984), “Refined modeling of reinforced concrete columns for seismic analysis”, EERC Report 84/03; Earthquake Engineering Research Center, University of California, Berkeley.

Lobo, P. S., Almeida, J. (2015), “RC fiber beam-column model with bond-slip in the vicinity of interior joints”, *Engineering structures*, **96**, 78-87.

Mahasuverachai, M. and Powell, G. H. (1982), “Inelastic analysis of piping and tubular structures”, Report UCB/EERC-82/27; Earthquake Engineering Research Center, University of California, Berkeley.

Menegotto M. and Pinto P. E. (1973), “Method of analysis for cyclically loaded reinforced concrete plane frames including changes in geometry and non-elastic behavior of elements under combined normal force and bending”, *IABSE symposium on resistance and ultimate deformability of structures acted on by well-defined repeated loads*, Lisbon, Portugal.

Monti, G. and Spacone, E. (2000), “Reinforced Concrete fiber beam element with bond slip”, *Journal of structural engineering* **126**(6), 654-661.

Popovics, S. (1973), “A numerical approach to the complete stress strain curve for concrete”, *Cement and Concrete Research,* **3**(5), 583-599.

Rajasankar, J. and Nagesh R. Iyer, (2009), “Modelling inelastic hinges using CDM for nonlinear analysis of reinforced concrete frame structures”, *Computers and Concrete,* **6**(4), 319-341.

Sabry, S., Gendy, F. M. and Ayoub, A. (2018), “Displacement and mixed fibre beam elements for modelling of slender reinforced concrete structures under cyclic loads”, *Engineering Structures,* **173**, 620-630.

Saritas, A. and Filippou, F. C. (2013), “Analysis of RC walls with a mixed formulation frame element”, *Computers and Concrete*, **12**(4), 519-536.

Souza, R. M. (2000), “Force-based Finite Element for Large Displacement Inelastic Analysis of Frames”, Ph.D. Dissertation, University of California at Berkeley, Berkeley, CA.

Spacone, E., Ciampi, V. and Filippou, F. C. (1992), “A beam element for seismic damage analysis”, EERC Report 92/08; Earthquake Engineering Research Center, University of California, Berkeley, CA.

Spacone, E., Filippou, F. C. and Taucer, F. F. (1996), “Mixed formulation of nonlinear beam finite element”, *Computers and Structures* **58,** 71-83.

Spacone, E., Filippou, F. C. and Taucer, F. F. (1996a), “Fiber beam-column model for non-linear analysis of R/C frames: Part I. Formulation”, *Earthquake Engineering Structural Dynamics,* **25**, 711-725.

Spacone, E., Filippou, F. C. and Taucer, F. F. (1996b), “Fiber beam-column model for non-linear analysis of R/C frames: Part II. Applications”, *Earthquake Engineering Structural Dynamics*, **25**, 727-742.

Taucer, F.F., Spacone, E. and Filippou, F.C. (1991), "A Fiber Beam-Column Element for Seismic Analysis of Reinforced Concrete Structures." EERC Report 91/17; Earthquake Engineering Research Center, University of California, Berkeley.

Tidemann, L., and Krenk, S. (2018), “A robust frame element with cyclic plasticity and local joint effects”, Engineering structures, **168**, 191-204.

Thomsen, J. H. and Wallace, J. W. (1995), ‘‘Displacement-Based Design of Reinforced Concrete Structural Walls: An Experimental Investigation of Walls with Rectangular and T-Shaped Cross-Sections’’, Report No. CU/CEE-95-06; Department of Civil and Environmental Engineering, Clarkson University, New York.

Zeris, C. A. (1986), “Three dimensional nonlinear response of reinforced concrete buildings”, Ph.D. Dissertation; University of California, Department of Civil Engineering, Berkeley.

Zeris, C.A. and Mahin, S. A. (1988), “Analysis of reinforced concrete beam-columns under uniaxial excitation”, *Journal of Structural Engineering* **114**, 804-820

Zeris, C. A. and Mahin, S. A. (1991), “Behavior of reinforced concrete structures subjected to biaxial excitation”, *Journal of Structural Engineering,* **117** (9), 2657-2673.